Peer-reviewed version available at *Appl. Sci.* **2020**, *10*, 819; doi:10.3390/app10030819

Article

High-Resolution Hologram Calculation Method Based on Light Field Image Rendering

Xin Yang [1,2], FuYang Xu [3], HanLe Zhang [1], HongBo Zhang [4], Kai Huang[3], Yong Li [3,*] and Qiong-Hua Wang [1,2,*]

[1] School of Instrumentation and Optoelectronic Engineering, Beihang University, Beijing 100191, China;
[2] Beijing Advanced Innovation Center for Big Data-based Precision Medicine, Beihang University, Beijing 100191, China; holooptics@buaa.edu.cn (X. Y.); hanlezhang@stu.scu.edu.cn (H. Z.)
[3] Institute of Information Optics, Zhejiang Normal University, Jinhua, Zhejiang 321004, China; xfy@zjnu.cn (F. X.); 727305480@qq.com (K. H.)
[4] Department of Computer and Information Sciences, Virginia Military Institute, Lexington 24450, VA, USA; zhangh@vmi.edu (H. Z.)
[*] Correspondence: liyong@zjnu.cn (Y. L.); qionghua@buaa.edu.cn (Q. H. W.)

Featured Application: The proposed method is applicable for static 3D advertising and holographic packaging.

Abstract: A fast calculation method for the full parallax high-resolution hologram is proposed based on the elemental light field image (EI) rendering. A 3D object located near the holographic plane is firstly rendered as multiple EIs with a pinhole array. Each EI is interpolated and multiplied by a divergent sphere wave and interfered with a reference wave to form a hogel. Parallel acceleration is used to calculate the high-resolution hologram because calculation of each hogel is independent. A high-resolution hologram with the resolution of 20,0000×20,0000 pixels is calculated only within 8 minutes. Full parallax high-resolution 3D displays are realized by optical reconstructions.

Keywords: holographic 3D display; computer generated holography; light field image rendering; pinhole array

1. Introduction

Holography can fully reconstruct 3D scene with all phase and amplitude information. The traditional optical holography can record very high-resolution hologram with laser as illumination but stable optical platform is needed as well as other optical devices. Different from the optical holography, the 3D information can be coded into a computer generated hologram for holographic 3D display [1,2]. Many efforts for dynamic holographic displays have been made for monochrome display or color display using laser or LED as illumination [3-8]. The progresses on dynamic holographic 3D display, however, still have proven difficult due to the constraints of limited bandwidth of current available spatial light modulator (SLM) and huge amount of calculation.

High-resolution holograms such as rainbow holograms and Fresnel holograms are applicable for 3D advertising and packaging because of the emerging of holographic printing technology [9-14]. The biggest challenge for high-resolution holography is the huge amount of computation. Multiple algorithms such as point cloud-based, layer-based, triangular mesh-based algorithms as well as the holographic stereogram methods have been proposed [15-18]. However, those methods are not effective for reducing the calculation burden for high-resolution hologram. We have proposed frequency fusing methods similar to holographic stereogram for full-parallax image hologram [11] and color rainbow hologram [10] calculation with high efficiency but the sizes of calculated holograms are limited by the RAM (Random Access Memory) of computer. Rectangular tiling algorithms have been proposed for high-resolution hologram calculation free of limitation from

computer RAM [19,20]. Taking the reference [19] as an example, each rectangular tile is calculated by using the 3D object data within the field of view (FOV) of this tile using point cloud-based method. A full-parallax hologram with a resolution of 20,000 × 20,000 can be up to 32.9 hours. Another rectangular tiling based algorithm is integral holography, which is the combination of integral imaging 3D display and holography [21-24]. In this method, each element light field image (EI) rendered from a micro-lens array or pinhole array is firstly fast Fourier transformed (FFT) as the complex amplitude of each elemental hologram or called hogel. And then the hogel is calculated by interference the complex amplitude with a reference wave. However, the calculation of complex amplitude using FFT is time consuming especially for large scale high-resolution hologram calculation.

In order to reduce the computational time of the high-resolution hologram and inspired from integral holography, a simple and fast calculation method without using FFT is proposed. A pinhole array is set behind the holographic plane for rendering EIs. Each EI located on the holographic plane is multiplied with a divergent spherical wave, which is regarded as the complex amplitude of this hogel. And a reference wave is interfered with complex amplitude for this hogel calculation. Parallel acceleration is used to speed up the calculation because the calculation of each hogel is independent. A full parallax high-resolution hologram with a resolution of 200,000 × 200,000 is calculated only within 8 minutes. The validity of this proposed method is approved by optical reconstructions.

2. Methods

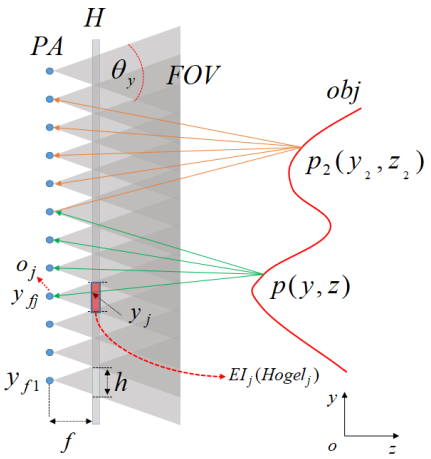

Figure 1. The rendering of EIs with a pinhole array for hologram calculation.

Figure 1 shows the rendering of EIs with a pinhole array for hologram calculation. PA is a pinhole array behind the holographic plane H. The distance between PA and H is *f*. obj is a 3D object in space and $p(y,z)$ and $p_2(y_2,z_2)$ are two object points of obj. The EI is an image rendered from the 3D object to a pinhole. Such as the EI_j, which is rendered from the pinhole O_j by calculating of the projected image from all 3D object to O_j within the opening angle from the pinhole to this EI. And this EI_j is coded into the $Hogel_j$. In this situation, the size of EI is the same as the size of hogel as well as their coordinates. The EI on holographic plane has a width of h and the FOV is depended on the opening angle θ_y of the EI to the corresponding pinhole in the y direction. Each EI is closely adjacent to other EIs. The coordinate of j-th pinhole o_j is y_{fj} and projections of point $p(y,z)$ and $p_2(y_2,z_2)$ within the FOV to each pinhole are demonstrated. The intersections of projection lines to each pinhole on holographic plane are coordinates of projected points of EI. Such as shown in Figure 1, y_{pj} is the coordinate of EI in the y direction, which can be expressed as:

$$y_{pj} = f\frac{y - y_{fj}}{z} + y_{fj}. \quad (1)$$

The calculation can also be applied to the x direction and x_{pi} of projected EI can be expressed as:

$$x_{pi} = f\frac{x - x_{fi}}{z} + x_{fi}, \tag{2}$$

where (x, y, z) is the coordinate of the object point P in 3D coordinate system and (x_{pi}, y_{pj}) is the coordinate of EI $im_{i,j}$ on holographic plane. (x_{fi}, y_{fj}) is the coordinate of the $(i\text{-}th, j\text{-}th)$ pinhole. The $(i\text{-}th, j\text{-}th)$ EI can be expressed as:

$$im_{i,j}(x_{pi}, y_{pj}) = A_p, \tag{3}$$

where A_p is the amplitude of object point $p(x, y, z)$. (i, j) is the index of the EI. The phase of this hogel on holographic plane is a phase of sphere wave from the pinhole to the hogel, which can be expressed as,

$$\mathrm{phs}_{i,j}(x_{pi}, y_{pj}) = \frac{2\pi}{\lambda}[\sqrt{(x_{pi} - x_{fi})^2 + (y_{pj} - y_{fj})^2 + f^2}]. \tag{4}$$

The complex amplitude of object wave-front corresponding to each hogel is the multiply of Eq. (3) by a divergent sphere wave with the phase illustrated in Eq. (4). This concept is simple and straightforward. From the view of local area, the local amplitude and spherical wave control the amplitude and propagation direction of this small beamlet.

Assuming that the reference light is a plane wave and the angle between the plane wave in the y direction and the z axis is θ_{refy}. The off-axis amplitude type $(i\text{-}th, j\text{-}th)$ hogel can be expressed as:

$$H_{i,j}(x_{pi}, y_{pj}) = im_{i,j}(x_{pi}, y_{pj})\cos[phs_{i,j}(x_{pi}, y_{pj}) - \frac{2\pi}{\lambda} y_{pj}\sin(\theta_{refy})]. \tag{5}$$

After the parameters of PA and FOV of the hologram as well as other necessary parameters are provided, each hogel can be calculated independently. And the all hogels form the final high-resolution hologram.

3. Experiment and results

The pixel pitch d_h of the hologram is 0.318 μm, which is determined by our holographic printer [9-11]. This principle of the home-made holographic printer is similar with the holographic printer introduced in reference [12], but the light source in our holographic printer is a blue LED with center wavelength of 365 nm rather than a laser. The max frequency that the holographic printer can be supported is $1/2d_h = 1573$ line/mm. Printing holograms at the highest resolution requires extremely stability for the printing system. In the practical usage, almost half of the highest resolution is used for hologram design. In the experiment, the diffraction angles of the FOV in the x and y directions are set as: θ_x is 48° and θ_y is 20°, respectively. And the angle of reference wave in the y direction and z axis is set as 22°. Assuming the wavelength is 632 nm. Therefore, the max frequency is $\sin(\theta_x/2)/\lambda = 643$ line/mm in the x direction and the max frequency is $\sin(\theta_y/2)/\lambda + \sin(\theta_{refy})/\lambda = 867$ line/mm in the y direction, respectively. Assuming the distance between pinhole and holographic plane is f=1 mm. In this situation, the width and length of each hogel or EI is $w = 2f\tan(\theta_x/2) = 0.89$ mm and $h = 2f\tan(\theta_y/2) = 0.35$ mm. The geometric relationship of the hologram calculation using a 3D point cloud model with two layers is shown in Figure 2(a). The first layer has a distance of 10 mm while the second layer has a distance 20 mm from the holographic plane H. The two layer Chinese characters are shifted in the vertical direction to guarantee not to overlap when they are viewed from the front view for simplicity. The 3D model has a size of 64 mm × 64 mm ×10 mm (W × H × D) with 984K object points. The front view of the 3D model is shown in Figure 2(b).

Preprints (www.preprints.org) | NOT PEER-REVIEWED | Posted: 17 January 2020 doi:10.20944/preprints201912.0195.v2

Peer-reviewed version available at Appl. Sci. 2020, 10, 819; doi:10.3390/app10030819

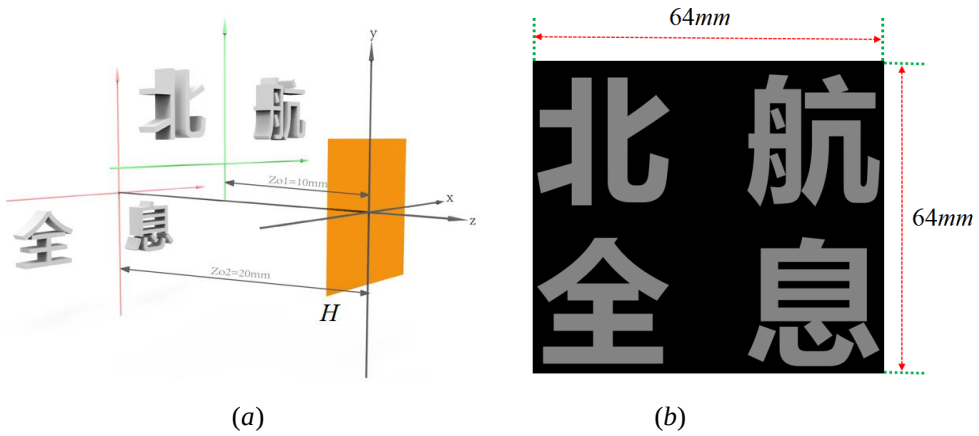

(*a*) (*b*)

Figure 2. The geometric relationship for hologram calculation: (a) The side view of the holographic plane H and 3D model; (b) The front view of the 3D model. The first layer Chinese characters are the abbreviation of "Beihang" university and the second layer Chinese characters mean "Holography".

Table 1. Parameters for hologram calculation.

Parameters	Values
Number of points in the 3D model	984K
Size of hologram	63.6 mm × 63.6 mm
Resolution of hologram	200K × 200K
Pixel pitch of hologram	0.318 μm
Resolution of hogel	2800 × 1108 pixels
Wavelength	632 nm
Size of EI	0.89 mm × 0.35 mm
Pixel pitch of EI	4 μm
Resolution of EI	222 × 88 pixels
Number of EIs	71 × 181

In the rendering of the EIs, the sampling intervals for both x and *y* directions are set as 4 μm and the resolution of each EI is 222 × 88 pixels. The parameters for hologram calculation are summarized in Table I. In the proposed method, the size of EI is the same as the size of hogel, but the sampling intervals are different. After we get an EI from the 3D model, this EI is firstly interpolated to a new EI with the same resolution as the hogel. The interpolated EI is used for hologram calculation according to Eq. (5). In the calculation, after the size of EI is determined, the number of EI is calculated by $63.6/0.89 = 71.46 \approx 71$ and $63.6/0.35 = 181.71 \approx 181$. The resolution 200K × 200K of the hologram is also approximation of the physic size of 63.6 mm × 63.6 mm. The approximation is possible because missing a little bit of data on the outer edge of the hologram does not affect the 3D display.

Figure 3(a) shows the rendered light field image, which contains all EIs rendered from the 3D model. Figure 3(b) is a partial enlarged light field image. The light field image almost has a resolution of 16K × 16K, which is much higher than the resolution of current commercially available display panels. The high-resolution light field image and high-resolution hologram guarantee high imaging quality and large FOV of reconstructed 3D image.

Because of the independent property of calculation for each hogel in the proposed method, "parfor" in Matlab is used for parallel acceleration. The MATLAB 2015b with a laptop (i7-9750HQ CPU, 16G RAM and 1024G SSD) is used for hologram calculation. Six CPU cores participate in the hologram calculation. The computational time is about 8 minutes for calculation of this hologram including the time used for the EIs rendering. The hologram is printed with our home-made holographic printer from Institute of Information Optics, Zhejiang Normal University about 4.5 hours.

Preprints (www.preprints.org) | NOT PEER-REVIEWED | Posted: 17 January 2020 doi:10.20944/preprints201912.0195.v2

Peer-reviewed version available at Appl. Sci. 2020, 10, 819; doi:10.3390/app10030819

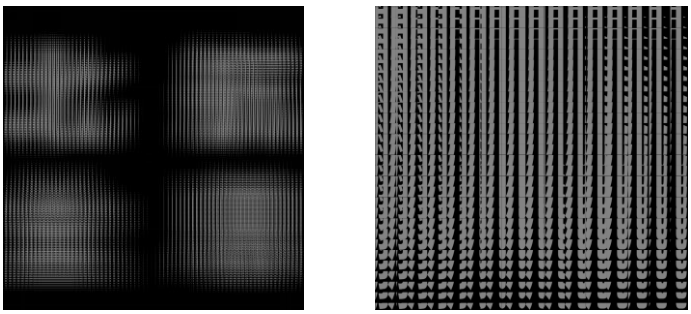

(*a*) (*b*)

Figure 3. The rendered light field image: (**a**) Light field image; (**b**) Partial enlarged part of (a).

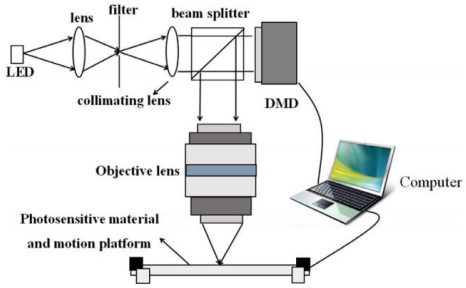

Figure 4. The diagram of holographic printer.

The overall diagram of the holographic printer is shown in Figure 4. The light from the LED is filtered and collimated to illuminate the digital micro mirror (DMD) with a resolution of 1024 × 768 pixels. A small portion of the calculated hologram with resolution of 600 × 600 pixels is first zeros padded to the same resolution as the DMD and then loaded into the DMD for display. The modulated light from DMD is imaged on the photosensitive material through the objective lens and this small portion hologram is printed. Controlled by computer, the motion platform is moved to the next position for printing the next hologram section. With this holographic printer, the maximum size of 200 mm × 200 mm hologram with pixel pitch of 0.318 μm can be printed on photoresist plate. The partial calculated hologram and the printed hologram are shown in Figures 5(a) and 5(b), respectively.

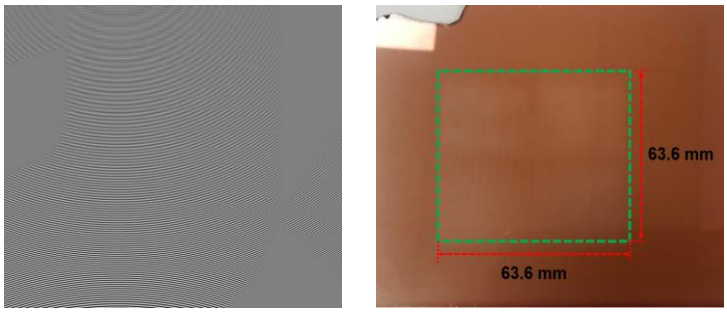

(*a*) (*b*)

Figure 5. Hologram for 3D display: (**a**) Partial calculated hologram; (**b**) Printed hologram.

In the reconstruction, a halogen lamp available in our lab is used as illumination source. The reconstruction of the hologram is demonstrated in Figure 6(a). The white light is coupled into the fiber and a divergent light from the fiber head illuminates the hologram H with a proper incline angle in the y direction. The diffracted light propagates into the human eye for watching the reconstructed 3D image. Real image in front of the hologram plane or virtual image behind the hologram plane can be watched by selecting a proper illumination angle. Figures 6(b)-6(d) show three reconstructed images from three different viewing angles. And the supplementary video I shows the reconstruction from different viewpoints.

Preprints (www.preprints.org) | NOT PEER-REVIEWED | Posted: 17 January 2020 doi:10.20944/preprints201912.0195.v2

Peer-reviewed version available at Appl. Sci. 2020, 10, 819; doi:10.3390/app10030819

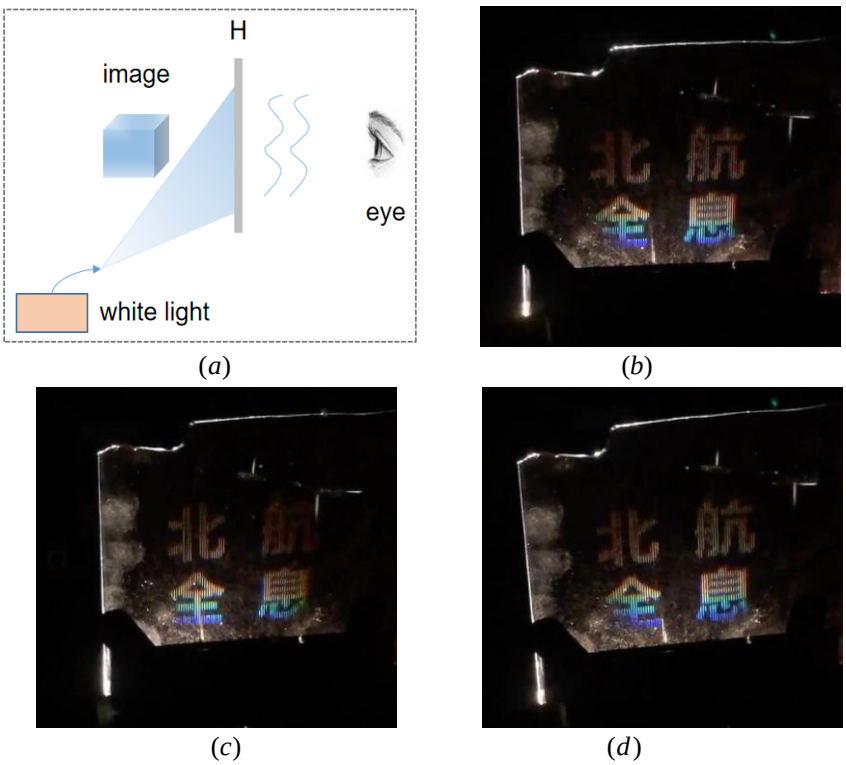

Figure 6. (**a**) The diagram of optical setup for reconstruction; (**b**)-(**d**) Different views of reconstructed 3D image. The supplementary video I shows the reconstruction from different viewpoints.

From the optical reconstruction, the parallax is smooth and the FOV is large. The brightness is a little difference due to the uneven incline illumination on this large area hologram. Figure 7 shows three images captured by our camera focusing on part of the holographic plane with different viewing angles. The two speckles in the red and green circles on the holographic plane are used as reference positions. From the results we can know that different perspective light coming from different position of the holographic plane, which is the core point of our method to encode the propagation of each pixel in EI to different angle with divergent sphere wave phase factor.

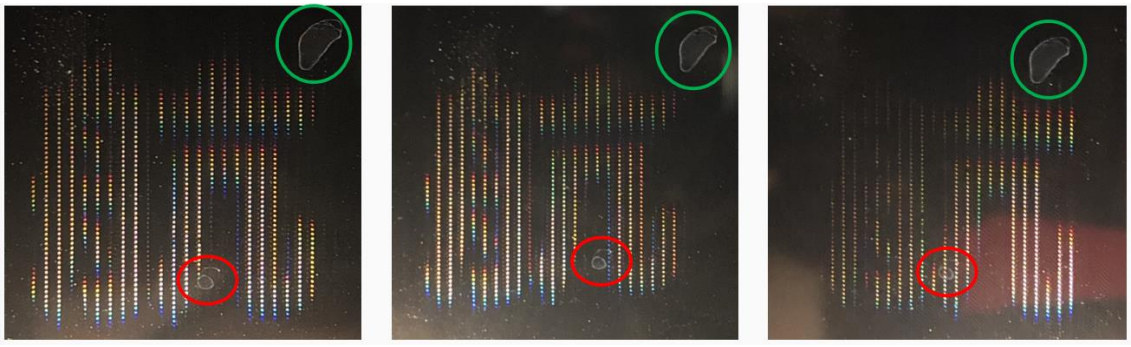

Figure 7. (**a**)-(**c**) Three different images captured by the camera focused on the holographic plane.

The large hogel size in the first experiment causes that human eyes can easily distinguish each hogel on the holographic plane. The 3D image viewed by the human eye is like watching through a fence. In order to reduce the fence effect and improve the quality of the displayed result, the second experiment is designed and carried out using the same model as the first experiment but with different parameters. In the second experiment, the distance between the pinhole array and holographic plane is $f = 0.25$ mm. In this situation, each hogel has a resolution of 700 × 277 pixels corresponding to the physic size of 0.22 mm × 0.09 mm. The sampling pitch in each EI is set as 1 μm and the resolution of each EI is 222 × 88 pixels, which is the same as in the first experiment. The

number of EIs is 287 × 725. The resolution of full light field image is about 63.7K × 63.7K in this experiment. Other parameters are all the same as the parameters of the first experiment. The calculation time of this hologram is approximate 37 minutes. Figure 8 shows the three reconstructed images. And the supplementary video II shows the 3D reconstruction from different viewing angles.

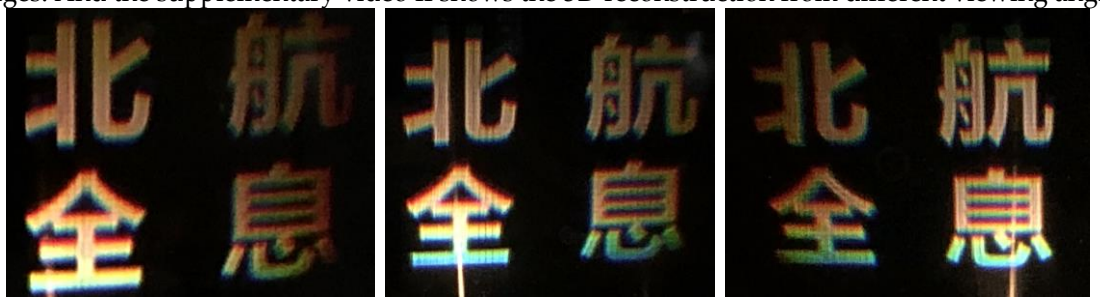

(*a*) (*b*) (*c*)

Figure 8. (**a**)-(**c**) Three reconstructed images from different viewpoints.
The supplementary video II shows the reconstruction from different viewpoints.

4. Discussion

To encode the high-resolution light field image into a high-resolution hologram has two important advantages: displaying of 3D image with higher resolution and the dramatically decreased calculation time of high-resolution hologram. In our proposed method, a pinhole array behind the holographic plane is used for EIs rendering and a divergent sphere wave is used as the phase information for each EI. However, the pinhole array can also be set in front of holographic plane and convergent sphere wave is used as phase information.

In the calculation, converting each EI to the complex amplitude information on each hogel plane using FFT is not needed in the proposed method. And the phase factor of divergent sphere wave is the same for all hogels, which means the phase factor is only needed to be calculated one time and reused for each hogel calculation. This direct encoding method can greatly reduce the computational time of high-resolution hologram.

In the encoding process of hologram, plane wave is used as reference wave for simplicity. Actually, a divergent sphere wave is more practical because the white light we used or a white light LED for illumination of the hologram is approximately a divergent wave. The reason why a white light can be used to reconstruct the hologram is that the distance between the reconstructed image and the holographic plane is near, similar to the case of the image holography, the color dispersion due to the white light illumination does not have a large influence on the reproduced 3D image. It should be noted that to display the hologram with laser as illumination is still possible with a higher resolution of reconstructed 3D image but speckle noise will exist.

we demonstrate two experiments for 3D display with different hogel size and sampling pitch. From the results, we can conclude that the calculation time is associated with the number of object points in the 3D model and EIs as well as the sampling interval in each EI. Well-designed parameters will guarantee high quality reconstructed image with a relative short computational time. The parallel computing using a GPU (graphics processing unit) is still possible for reduction of computational time further.

The displayed results with white light as illumination is a grayscale 3D display. However, the concept of full color rainbow holography [9,12] can also be applied to our method for full color 3D display at the cost of losing vertical parallax.

In the proposed method, the resolution of each EI and size of EI or hogel are related, which means a large FOV will cause large hogel size and lead to more fence effect. A large depth 3D display is not possible with this method because the image far from the holographic plane will be blur due to the white light illumination. However, the proposed method is still valuable for holographic packing or 3D display purpose with relative small depth.

5. Conclusion

In this study, a simple and fast method for full parallax high-resolution holographic 3D display is demonstrated without using FFT. The encoding of the high-resolution light field image with holographic method to speed up the calculation is the essence of our method. A high-resolution hologram with 40 billion pixels is calculated only within 8 minutes and the optical 3D reconstruction is effectively approved by experiments.

Author Contributions: X. Y. wrote the program for hologram calculation and completed the relevant experiments; H. Z. and F. X. rendered the light field images and printed the hologram; H. Z. helped to discuss the research and modified the document; K. H. helped to prepare data for printing; Y. L. and Q.-H. W. led the project and provided supports.

Funding: This research was funded by National Key R&D Program of China, under Grant No. 2017YFB1002900 and by National Natural Science Foundation of China under Grant No. 61927809.

Conflicts of Interest: The authors declare no conflict of interest.

References

1. F. Yaras, H. Kang, and L. Onural. State of the art in holographic display: A survey. J. Disp Technol., **2010**, 6(10), 443-454.
2. K. Matsushima, Y. Arima, and S. Nakahara. Digitized holography: modern holography for 3D imaging of virtual and real objects. Appl. Opt., **2011**, 50(34), H287-H284.
3. X. Yang, H. Zhang, and Q. W. A fast-computer-generated holographic method for VR and AR near-eye 3D display. Appl. Sci., **2019**, 9, 4164: 1-11.
4. S. Lin, D. Wang, Q. Wang, E. Kim. Full-color holographic 3D display system using off-axis color-multiplexed-hologram on single SLM. Opt. Laser Eng., **2020**, 126, 105895:1-9.
5. A. Maimone, A. Georgiou, and J. Kollin. Holographic near-eye displays for virtual and augmented reality. ACM Trans. Graph., **2017**, 36, 8501-8516.
6. X. Li, J. Liu, T. Zhao, and Y. Wang. Color dynamic holographic display with wide viewing angle by improved complex amplitude modulation. Opt. Express, **2018**, 26, 2349-2358.
7. H. Gao, F. Xu, J. Liu, Z. Dai, W. Zhou, S. Li, Y. Yu, and H. Zheng. Holographic three-dimensional virtual reality and augmented reality display based on 4K-spatial light modulators. Appl. Sci., **2019**, 9, 1128:1-9.
8. S. Lin, H. Cao, and E. Kim. Single SLM full-color holographic three-dimensional video display based on image and frequency-shift multiplexing. Opt. Express, **2019**, 27, 15926-15942.
9. Y. Shi, H. Wang, Y. Li, H. Jin, and L. Ma. Practical method for color computer generated rainbow holograms of real-existing objects. Appl. Opt., **2009**, 48, 4219-4226.
10. X. Yang, H. Wang, Y. Li, F. Xu, H. Zhang and J. Zhang. Large scale and high resolution computer-generated synthetic color rainbow hologram. J. Opt., **2019**, 21, 025601: 1-10.
11. X. Yang, H. Wang, Y. Li, F. Xu, H. Zhang, J. Zhang, and Q. Yan. Computer generated full-parallax synthetic hologram based on frequency mosaic. Opt. Commun., **2019**, 430, 24-30.
12. T. Yamaguichi, and H. Yoshikawa. High resolution computer generated rainbow hologram. Appl. Sci., **2018**, 8, 1955:1-11.
13. O. Kunieda, and K. Matsushima. High-quality full-parallax full-color three-dimensional image reconstructed by stacking large-scale computer-generated volume holograms. Appl. Opt., **2019**, 58, G104-G111.
14. Y. Yamamoto, H. Nakayama, N. Takada, T. Nishitsuji, T. Sugie, T. Kakue, T. Shimobaba, and T. Ito. Large-scale electroholography by HORN-8 from a point-cloud model with 400,000 points. Opt. Express, **2018**, 26, 34259-34265.
15. P. Su, W. Cao, J. Ma, B. Cheng, X. Liang, L. Cao, and G. Jin. Fast computer-generated hologram generation

method for three-dimensional point cloud model. J. Display Technol., **2016**, 12, 1688-1694.

16. D. Arai, T. Shimobaba, K. Murano, Y. Endo, R. Hirayama, D. Hiyama, T. Kakue, and T. Ito. Acceleration of computer-generated holograms using tilted wavefront recording plane method. Opt. Express, **2015**, 23, 1740-1747.
17. J. Liu and H. Liao. Fast occlusion processing for a polygon-based computer-generated hologram using the slice-by-slice silhouette method. Appl. Opt., **2018**, 57, A215-A221.
18. D. Abookasis and J. Rosen. Three types of computer-generated hologram synthesized from multiple angular viewpoints of a three-dimensional scene. Appl. Opt., **2006**, 45, 6533-6538.
19. H. Zhang, Y. Zhao, L. Cao, and G. Jin. Fully computed holographic stereogram based algorithm for computer-generated holograms with accurate depth cues. Opt. Express, **2015**, 23, 3901-3913.
20. D. Blinder, and T. Shimobaba. Efficient algorithms for the accurate propagation of extreme-resolution holograms. Opt. Express, **2019**, 27, 29905-29915.
21. H. Zhang, H. Deng, J. Li, M. He, D. Li, and Q. H. Wang. Integral imaging-based 2D/3D convertible display system by using holographic optical element and polymer dispersed liquid crystal. Opt. Lett., **2019**, 44, 387-390.
22. Y. Zhang, Y. Fu, H. Wang, H. Li, S. Pan, and Y. Du. High resolution integral imaging display by using a microstructure array. J. Opt. Technol., **2019**, 86, 100-104.
23. L. Ai, H. Cao, H. Sun, and X. Shi. Performance enhancement of integral imaging based Fresnel hologram capturing by the intermediate view reconstruction. Opt. Express, **2019**, 27, 31942-31955.
24. X. Zhang, G. Lv, Z. Wang, Z. Hu, S. Ding, and Q. Feng. Resolution-enhanced holographic stereogram based on integral imaging using an intermediate-view synthesis technique. Opt. Commun., **2020**, 457, 124656:1-6.